



**HAL**  
open science

## Purification and Quality Control of Recombinant Septin Complexes for Cell-Free Reconstitution

Gerard Castro-Linares, Jeffrey den Haan, Francois Iv, Carla Silva Martins, Aurélie Bertin, Manos Mavrakis, Gijsje H Koenderink

► **To cite this version:**

Gerard Castro-Linares, Jeffrey den Haan, Francois Iv, Carla Silva Martins, Aurélie Bertin, et al.. Purification and Quality Control of Recombinant Septin Complexes for Cell-Free Reconstitution. Journal of visualized experiments: JoVE, 2022, 184, 10.3791/63871 . hal-03703833v2

**HAL Id: hal-03703833**

**<https://cnrs.hal.science/hal-03703833v2>**

Submitted on 5 Jul 2022

**HAL** is a multi-disciplinary open access archive for the deposit and dissemination of scientific research documents, whether they are published or not. The documents may come from teaching and research institutions in France or abroad, or from public or private research centers.

L'archive ouverte pluridisciplinaire **HAL**, est destinée au dépôt et à la diffusion de documents scientifiques de niveau recherche, publiés ou non, émanant des établissements d'enseignement et de recherche français ou étrangers, des laboratoires publics ou privés.

1 **TITLE:**  
2 Purification and Quality Control of Recombinant Septin Complexes for Cell-Free Reconstitution  
3

4 **AUTHORS AND AFFILIATIONS:**

5 Gerard Castro-Linares<sup>1</sup>, Jeffrey den Haan<sup>1</sup>, Francois Iv<sup>2</sup>, Carla Silva Martins<sup>2</sup>, Aurélie Bertin<sup>3</sup>,  
6 Manos Mavrakis<sup>2</sup>, Gijsje H. Koenderink<sup>1</sup>  
7

8 <sup>1</sup>Department of Bionanoscience, Kavli Institute of Nanoscience Delft, Delft University of  
9 Technology, 2629 HZ Delft, The Netherlands

10 <sup>2</sup>Institut Fresnel, CNRS UMR7249, Aix Marseille Univ, Centrale Marseille, 13013 Marseille, France

11 <sup>3</sup>Institut Curie, Université PSL, Sorbonne Université, CNRS UMR 168, Laboratoire Physico Chimie  
12 Curie, 75005 Paris, France  
13

14 Corresponding authors:

15 Aurélie Bertin ([Aurelie.Bertin@curie.fr](mailto:Aurelie.Bertin@curie.fr))

16 Manos Mavrakis ([manos.mavrakis@fresnel.fr](mailto:manos.mavrakis@fresnel.fr))

17 Gijsje H. Koenderink ([G.H.Koenderink@tudelft.nl](mailto:G.H.Koenderink@tudelft.nl))  
18

19 Email addresses of co-authors:

20 Gerard Castro-Linares (G.CastroLinares@tudelft.nl)

21 Jeffrey den Haan (J.C.A.DenHaan-1@tudelft.nl)

22 Francois Iv (iv.francois@yahoo.fr)

23 Carla Silva Martins (silva-martins@fresnel.fr)  
24

25 **SUMMARY:**

26 *In vitro* reconstitution of cytoskeletal proteins is a vital tool to understand the basic functional  
27 properties of these proteins. The present paper describes a protocol to purify and assess the  
28 quality of recombinant septin complexes, which play a central role in cell division and migration.  
29

30 **ABSTRACT:**

31 Septins are a family of conserved eukaryotic GTP-binding proteins that can form cytoskeletal  
32 filaments and higher-order structures from hetero-oligomeric complexes. They interact with  
33 other cytoskeletal components and the cell membrane to participate in important cellular  
34 functions such as migration and cell division. Due to the complexity of septins' many interactions,  
35 a large number of septin genes (13 in humans), and the ability of septins to form hetero-  
36 oligomeric complexes with different subunit compositions, cell-free reconstitution is a vital  
37 strategy to understand the basics of septin biology. The present paper first describes a method  
38 to purify recombinant septins in their hetero-oligomeric form using a two-step affinity  
39 chromatography approach. Then the process of quality control used to check for purity and  
40 integrity of the septin complexes is detailed. This process combines native and denaturing gel  
41 electrophoresis, negative stain electron microscopy, and interferometric scattering microscopy.  
42 Finally, a description of the process to check for the polymerization ability of septin complexes  
43 using negative stain electron microscopy and fluorescent microscopy is given. This demonstrates

44 that it is possible to produce high-quality human septin hexamers and octamers containing  
45 different isoforms of septin\_9, as well as *Drosophila* septin hexamers.

46

#### 47 **INTRODUCTION:**

48 The cytoskeleton has been classically described as a three-component system consisting of actin  
49 filaments, microtubules, and intermediate filaments<sup>1</sup>. But recently, septins have been  
50 acknowledged as a fourth component of the cytoskeleton<sup>1</sup>. Septins are a family of GTP-binding  
51 proteins that are conserved in eukaryotes<sup>2</sup>. Septins are involved in many cellular functions such  
52 as cell division<sup>3</sup>, cell-cell adhesion<sup>4</sup>, cell motility<sup>5</sup>, morphogenesis<sup>6</sup>, cellular infection<sup>7</sup>, and the  
53 establishment and maintenance of cell polarity<sup>8</sup>. Despite their important functions, how septins  
54 are involved in such processes is poorly understood.

55

56 The septin family of proteins is subdivided into several subgroups (four or seven, depending on  
57 the classification) based on protein sequence similarity<sup>2</sup>. Members of different subfamilies can  
58 form palindromic hetero-oligomeric complexes that are the building blocks of filaments, which  
59 in turn assemble into higher-order structures such as bundles, rings, and meshworks<sup>1,9-12</sup>. Further  
60 molecular complexity arises from the presence of different splice variants, an example being  
61 human SEPT9, where there is evidence for specific functions of different splice variants<sup>13-15</sup>.  
62 Additionally, the length of the hetero-oligomers depends on species and cell type. For instance,  
63 *Caenorhabditis elegans* septins form tetramers<sup>16</sup>, *Drosophila melanogaster* septins form  
64 hexamers<sup>17</sup> (**Figure 1A**), *Saccharomyces cerevisiae* septins form octamers<sup>18</sup>, and human septins  
65 form both hexamers and octamers<sup>19</sup> (**Figure 1A**). The ability of septin isoforms and splice variants  
66 from the same subfamily to substitute each other in the complex and the (co-)existence of  
67 differently sized hetero-oligomers have made it difficult to delineate the cellular functions of  
68 different hetero-oligomeric complexes<sup>12</sup>.

69

70 Another interesting ability of septins is their ability to interact with many binding partners in the  
71 cell. Septins bind the plasma membrane and membranous organelles during interphase and cell  
72 division<sup>20-22</sup>. In dividing cells, septins cooperate with anillin<sup>23-25</sup> and actin and myosin during  
73 cytokinesis<sup>26,27</sup>. At the late stages of cytokinesis, septins seem to regulate the endosomal sorting  
74 complexes required for transport (ESCRT) system for midbody abscission<sup>28</sup>. Additionally, there is  
75 also evidence of septin located on the actin cortex and actin stress fibers of cells in interphase  
76 cells<sup>29-31</sup>. In specific cell types, septins also bind and regulate the microtubule cytoskeleton<sup>32,33</sup>.

77

78 All of these features make septins a very interesting protein system to study, but also a  
79 challenging one. The combination of a large number of septin subunits (13 genes in humans  
80 without counting splice variants<sup>2</sup>) with the potential of septin subunits from the same subfamily  
81 to substitute each other and form differently sized hetero-oligomers makes it difficult to draw a  
82 conclusion on the cellular function of a specific septin by genetic manipulation. Furthermore, the  
83 multiple interactions of septins make interpreting the effects of common research tools such as  
84 drugs<sup>34</sup> directed at cytoskeletal or membrane components a hard task.

85

86 A way to overcome this situation is to complement research in cells with *in vitro* (cell-free)  
87 reconstitution of septins. *In vitro* reconstitution allows for the isolation of a single type of septin

88 hetero-oligomers with a specific subunit composition and length<sup>18,35–37</sup>. This complex can then  
89 be studied in a controlled environment, either alone, to discover the basic structural and  
90 physicochemical properties of septins<sup>38–40</sup>, or in combination with desired partners such as model  
91 biomembranes<sup>11,41,42</sup>, actin filaments<sup>10,27</sup>, or microtubules<sup>32,36</sup>, to decipher the nature of their  
92 interactions.

93

94 Therefore, a reliable method to purify different septin complexes efficiently is vital for septin  
95 research. However, even using the same protocol, different purifications can give proteins with  
96 different activity/functionality or even integrity. For commercially available proteins such as  
97 enzymes, the functionality and enzymatic activity are carefully validated<sup>43</sup>. Implementing careful  
98 quality control for cytoskeletal or structural proteins such as septins can be challenging, but it is  
99 essential to make experiments across labs comparable.

100

101 This paper describes a robust method to purify high-quality recombinant septins in their hetero-  
102 oligomeric form based on the simultaneous expression of two vectors containing mono- or bi-  
103 cistronic constructs (**Table 1**) in *Escherichia coli* cells. The method consists of a two-step affinity  
104 chromatography approach to capture septin hetero-oligomers containing both a his<sub>6</sub>-tagged  
105 septin and a Strep-II-tagged septin (**Figure 1B,C**). This protocol, first described in Iv et al.<sup>10</sup>, has  
106 been used to purify *Drosophila* septin hexamers<sup>11,27,35</sup>, human septin hexamers<sup>10</sup>, and several  
107 human septin octamers containing different native (isoform 1, 3, and 5)<sup>10,32</sup> or mutated SEPT9  
108 isoforms<sup>32</sup>. Furthermore, a description of a set of techniques to assess the quality of the purified  
109 septins is given. First, the integrity and correct stoichiometry of the septin subunits is checked  
110 using denaturing electrophoresis and transmission electron microscopy (TEM). Then, to check for  
111 the presence of hetero-oligomers of the correct molecular mass and to test for the presence of  
112 monomers or smaller oligomers indicative of complex instability is examined by native  
113 electrophoresis and mass photometry *via* Interferometric scattering microscopy (iSCAT). Finally,  
114 the last step consists of the assessment of the polymerizing activity of the septins using  
115 fluorescence microscopy and TEM.

116

117 [Place **Figure 1** here]

118

## 119 **PROTOCOL:**

120

### 121 **1. Purification of septin hetero-oligomers**

122

#### 123 1.1. Co-transformation of bacterial cells with the expression vectors

124

125 1.1.1. Select a combination of one pnEA and one pnCS plasmid<sup>44</sup> that will be used for expression.  
126 Choose the combination depending on the desired subunit composition of the septin hetero-  
127 oligomer<sup>10,35</sup> and whether or not fluorescent tagging is required.

128

129 NOTE: C-terminally tagged monomeric superfolder GFP (msfGFP)-tagged SEPT2 (for human  
130 septins) or msfGFP- or monomeric enhanced GFP (mEGFP)-Dsep2 (for *Drosophila* septins) is used  
131 (**Table 1**).

132  
133 1.1.2. Pipette 1  $\mu\text{L}$  of each plasmid ( $\sim 1 \text{ ng}/\mu\text{L}$ ) in 100  $\mu\text{L}$  of competent BL21 *Escherichia coli* cells  
134 and incubate on ice for 20 min.  
135  
136 1.1.3. Place the cells in a water bath at 42  $^{\circ}\text{C}$  for 40 s and then immediately incubate them for 3  
137 min on ice.  
138  
139 1.1.4. Add 0.9 mL of lysogeny broth (LB) medium to the cell suspension and let the cells grow for  
140 1 h at 37  $^{\circ}\text{C}$ . Plate 100  $\mu\text{L}$  of cells on warm LB-agar plates containing 100  $\mu\text{g}/\text{mL}$  of ampicillin and  
141 100  $\mu\text{g}/\text{mL}$  spectinomycin and incubate overnight at 37  $^{\circ}\text{C}$ .  
142  
143 1.2. Grow bacterial pre-culture  
144  
145 1.2.1. Fill a 250 mL Erlenmeyer flask with 100 mL of Terrific broth (TB) or LB medium containing  
146 100  $\mu\text{g}/\text{mL}$  of ampicillin and 100  $\mu\text{g}/\text{mL}$  spectinomycin.  
147  
148 1.2.2. Pick out a single colony from the LB-agar plate with a sterile inoculation loop and transfer  
149 it to fresh media from step 1.2.1.  
150  
151 1.2.3. Incubate at 37  $^{\circ}\text{C}$  in a rotary shaker incubator, either overnight (o/n) or for at least 6 h.  
152  
153 NOTE: From this culture, a glycerol stock can be prepared by mixing the bacterial suspension 1:1  
154 with glycerol and stored at -80  $^{\circ}\text{C}$ . This stock can be used in step 1.2.2 instead of a freshly  
155 transformed colony.  
156  
157 1.3. Bacterial culture and protein expression induction  
158  
159 1.3.1. Transfer 100 mL of grown bacteria into 5 L of TB or LB containing 50  $\mu\text{g}/\text{mL}$  of ampicillin  
160 and 50  $\mu\text{g}/\text{mL}$  spectinomycin.  
161  
162 1.3.2. Grow this culture at 37  $^{\circ}\text{C}$  in a shaker incubator until it reaches an optical density (OD)  
163 measured at a wavelength of 600 nm in the range of 2-3 for unlabeled septins or 0.6-0.8 for  
164 msfGFP/mEGFP-labelled septins and induce protein expression by adding a final concentration  
165 of 0.5 mM IPTG. The lower OD for the labeled septins is to avoid reaching the death phase in their  
166 longer expression time, as detailed in the next step.  
167  
168 1.3.3. Incubate the cells expressing unlabeled septin hetero-oligomers for 3 h at 37  $^{\circ}\text{C}$  or the cells  
169 expressing msfGFP-labelled hetero-oligomers overnight at 17  $^{\circ}\text{C}$ .  
170  
171 NOTE: The short protein expression time for unlabeled complexes, facilitated by the use of the  
172 richer TB medium, is chosen to prevent protein degradation. The longer expression time  
173 combined with lower temperature for labelled complexes is chosen to allow for correct folding  
174 of the msfGFP tag.  
175

176 1.4. Bacterial lysis and lysate clarification

177

178 NOTE: From this point onwards in the purification procedure, keep the protein-containing  
179 solution on ice or at 4 °C at all times, to prevent proteolytic protein degradation or loss of activity.

180

181 1.4.1. Collect the cultured cells by centrifuging at 4000 x *g* for 20 min at 4 °C. Discard the  
182 supernatant.

183

184 1.4.1.1. Optionally, snap-freeze the pellet in this step and store at -80 °C for around 6 months. If  
185 this option is chosen, make sure to thaw the pellet on ice **before continuing**.

186

187 1.4.2. Dissolve the pellet in 100 mL of lysis buffer (**Table 2**) and lyse the cells. Choose one of the  
188 two options below

189

190 1.4.2.1. Sonicate in 7 cycles of 30 s ON and 59 s OFF with a tip sonicator using 30% amplitude  
191 (note that the settings are sonicator-dependent).

192

193 1.4.2.2. Break down the cells in the French press by passing them at least 3x.

194

195 1.4.3. Clarify the cell lysate by centrifuging at 20,000 x *g* for 30 min at 4 °C and keep the  
196 supernatant. It is recommended to start with step 1.5.1 during this centrifugal step.

197

198 1.4.4. Optionally, take a sample for denaturing electrophoresis as described in section 2.

199

200 1.5. Affinity chromatography for His-tagged proteins

201

202 NOTE: This step yields complexes containing human SEPT2 or *Drosophila* Sep1 using a nickel  
203 column (**Figure 1B**).

204

205 1.5.1. Equilibrate a pre-packed nickel sepharose high-performance chromatography column with  
206 septin buffer (**Table 2**).

207

208 1.5.2. Load the clarified supernatant onto the column at 1 mL/min and wash the bound protein  
209 with at least three column volumes of septin buffer.

210

211 1.5.3. Elute the septin complexes with 50% HisTrap elution buffer (**Table 2**), to yield an imidazole  
212 concentration of 250 mM, at 1 mL/min while collecting 0.5 mL fractions.

213

214 1.5.4. Pick the fractions containing septin complexes as indicated by the optical absorbance of  
215 the eluate at 280 nm monitored online with a fast protein liquid chromatography (FPLC) system  
216 or after the purification with a microvolume spectrophotometer.

217

218 NOTE: Imidazole absorbs light at 280 nm. This probably explains why the protein peak does not  
219 go back to zero absorbance after the septin elution (**Figure 2A**).

220

## 221 1.6. Affinity chromatography for Strep-II-tagged proteins

222

223 NOTE: This step yields complexes containing either human SEPT7 (hexamers), human SEPT9  
224 (octamers), or *Drosophila* Peanut using a Strep-Tactin column (**Figure 1B**). The chromatography  
225 column is based on a modified biotin-streptavidin system. The protein is tagged with modified  
226 biotin (Strep-II-tag) and the column contains an engineered streptavidin (Strep-Tactin). Despite  
227 being modified from the biotin-streptavidin system, there is no interference between the the  
228 Strep-Tactin-Strep-II-tag system, and the biotin-streptavidin system. The described system is  
229 used to avoid interference with reconstitution assays using biotin and streptavidin.

230

231 1.6.1. Equilibrate a pre-packed StrepTactin sepharose high-performance chromatography  
232 column with septin buffer (**Table 2**).

233

234 1.6.2. Load the septin-containing fractions recovered from the nickel column at 1 mL/min and  
235 wash the bound protein with at least three column volumes of septin buffer.

236

237 1.6.3. Elute the septin complexes with 100% StrepTrap elution buffer (**Table 2**), to yield a  
238 concentration of 2.5mM desthiobiotin, at 1 mL/min while collecting 0.5 mL fractions.

239

240 NOTE: The desthiobiotin in the StrepTrap elution buffer must be dissolved fresh.

241

242 1.6.4. Pick the fractions containing septin complexes as indicated by the optical absorbance of  
243 the eluate at 280 nm monitored online with an FPLC system or after the purification with a  
244 microvolume spectrophotometer.

245

246 NOTE: The denaturing electrophoresis is usually done at this point with samples of the column  
247 washings and septin fractions. The order of columns can be inverted with indistinguishable  
248 results, i.e., the clarified lysate after step 1.4 can be subjected to Strep-Tactin affinity  
249 chromatography followed by nickel affinity chromatography.

250

## 251 1.7. Dialysis and storage

252

253 1.7.1. To remove the desthiobiotin from the final storage solution, dialyze the septin complexes  
254 in a ~1:300 sample-to-buffer volume ratio against septin buffer (**Table 2**) supplemented with 1  
255 mM DTT overnight, or for at least 4 h, at 4 °C using a 30 kDa MWCO dialysis membrane.

256

257 1.7.2. Optionally, concentrate the septins using a 30 kDa MWCO centrifugal concentration  
258 column up to the desired concentration. Aim for a concentration of 5-7  $\mu$ M, as measured *via* the  
259 solution optical absorbance at 280 nm and using a theoretical extinction coefficient calculated  
260 *via* ProtParam (**Table 3**).

261

262 1.7.3. Aliquot the protein complexes into the desired aliquot size, snap-freeze the aliquot, and  
263 store it at -80 °C.

264

265 NOTE: It is recommended to not store the protein more than 6 months. In addition, it is  
266 recommended to perform regular quality control experiments, especially if the protein is stored  
267 longer than the recommended time.

268

## 269 **2. Quality control of purity and integrity of septin hetero-oligomer**

270

271 NOTE: The hetero-oligomer quality control consists of a set of biochemical and imaging  
272 techniques that allow for the detection of the mass and integrity of the septin complexes present  
273 in the solution.

274

275 2.1. Stoichiometric ratio of septin subunits *via* denaturing electrophoresis to check for the  
276 formation of the septin hetero-oligomer with the correct components.

277

278 2.1.1. Mix 10  $\mu\text{L}$  of the selected fractions with 10  $\mu\text{L}$  of 2x SDS sample buffer, load them onto a  
279 precast 4%-15% TGX gel, and fill the system with Tris/glycine/SDS running buffer.

280

281 2.1.2. Run the electrophoresis for 35 min at 200 V and stain the gel with InstantBlue to visualize  
282 the results. Molecular weights of the individual septin proteins and septin hetero-oligomeric  
283 complexes can be found in **Table 3**.

284

285 **2.1.3.** Measure the relative intensity of each band inside each lane containing purified septins in  
286 a contrast inverted image. Do this by calculating the mean intensity of equally sized rectangles  
287 around each band and of an equally sized rectangle on a region without any band in the same  
288 lane. Then, normalize the values by dividing the intensity of each band by the intensity of the  
289 region without bands.

290

291 NOTE: If the intensity is saturated (for example, values of 255 for an 8-bit image on a contrast  
292 inverted image), skip the lane.

293

294 2.2. Ensemble-averaged native size distribution *via* native electrophoresis

295

296 2.2.1. Prepare 800mL of anode buffer and 200mL of light blue cathode buffer the day before and  
297 store them in the fridge. To prepare the anode buffer dilute 40mL of 20x running buffer with  
298 760mL of type-I deionized water (I-water). To prepare the light blue cathode buffer dilute 10mL  
299 of 20x running and 1mL of 20x cathode additive with 189mL of I-water.

300

301 2.2.2. Prepare 10  $\mu\text{L}$  of the sample by mixing  $\sim 500$  ng of septin with the needed amount of sample  
302 buffer (2.5  $\mu\text{L}$  in this case, due to the use of a 4x sample buffer; see **Table of Materials**), and I-  
303 water enough to reach a volume of 10  $\mu\text{L}$ .

304

305 2.2.3. Load the samples onto the gel and fill the system with the ice-cold anode and cathode  
306 buffers.

307



308 2.2.4. Run the electrophoresis for around 115 min at 150 V with a power supply that does not  
309 stop at low currents and stain the gel with InstantBlue to visualize the results. Molecular weights  
310 of the single proteins and complexes calculated based on the sequence can be found in **Table 3**.  
311

312 2.3. Single-molecule mass distribution using mass photometry *via* interferometric scattering  
313 microscopy  
314

315 2.3.1. Wash #1.5 glass slides by sonicating them in an ultrasonic cleaner for 5 min in I-water, 5  
316 min in isopropanol, and finally 5 min in I-water.  
317

318 2.3.2. Dry two glass slides with a gentle stream of nitrogen gas and place a 7  $\mu$ L drop of 0.01%  
319 Poly-lysine (PLL) solution on the center of one of the slides. Then, place the center of the other  
320 slide on top of the PLL drop, orienting the two slides orthogonally for easy separation. Incubate  
321 for 30 s.  
322

323 2.3.2.1. Wash by immersing in a beaker with I-water once, and by directly applying a stream of I-  
324 water twice. Then dry the two slides with a flow of nitrogen gas. These slides can be stored  
325 afterward for around 6 weeks at room temperature in dry conditions.  
326

327 NOTE: Label the side of the slide that is treated with the PLL-PEG to correctly run the experiment.  
328

329 2.3.3. Just before the experiment, cut a piece of 2x2, 3x2, or 3x3 gaskets (to yeild 4, 6, or 9  
330 imaging chambers/slide, respectively) and stick it on the PLL-PEG treated part of a glass slide  
331 while avoiding the glass slide and the gaskets to contact any dirty surface. Place the slide on a  
332 light-duty wiper tissue and press on the gaskets with a pipette tip to stick them while there is still  
333 the protecting plastic on the gaskets.  
334

335 2.3.4. Warm septin buffer (**Table 2**) to room temperature and thaw the proteins in hand (keep  
336 them on ice afterward).  
337

338 NOTE: iSCAT shows the signal of some detergents and small molecules that resemble protein  
339 signals<sup>45</sup>. DTT is one of those small molecules and that is why it is not used for this experiment.  
340 There is only a trace of DTT coming from the stored septin.  
341

342 2.3.5. Place the slide with gaskets on the commercial mass photometry system containing 19  $\mu$ L  
343 of septin buffer and focus the microscope using the autofocus option. Follow the manufacturer's  
344 instructions to check if the found focus is correct. Optimize the frame rate and the exposure time  
345 by pressing on **Optimize illumination** and refocus with the autofocus option with the new  
346 settings. The standard 100x objective that is part of the setup is used.  
347

348 2.3.6. Create or load a project folder to store the data using **File > New Project** or **File > Load**  
349 **Project**.  
350

351 2.3.7. Pipette 1  $\mu\text{L}$  of sample on the 19 $\mu\text{L}$  buffer drop used to focus and mix while minimizing the  
352 movement of the slide by not touching anything while doing so. Then record a 6000-frame video  
353 by pressing on **Record**.

354  
355 2.3.7.1. For correct analysis, record the following samples: septin buffer, protein mass standard  
356 for the calibration of the signal-to-mass ratio (if a recent calibration is available and the  
357 environmental conditions have not changed, this sample can be skipped), and 250 nM of septin  
358 complexes diluted in septin buffer without DTT (this gives a final concentration of  $\sim 12.5$  nM).

359  
360 2.3.8. Analyze the videos using the manufacturer's software to obtain the protein mass  
361 distribution. Check for good quality data as follows.

362  
363 2.3.8.1. If peaks of different septin hetero-oligomers sizes are overlapping too much or too many  
364 events are detected ( $>3500$  events for a 6000-frames video with the regular field of view of 128  
365 pixels x 34 pixels spanning 10.8  $\mu\text{m}$  x 2.9  $\mu\text{m}$ ), decrease the final septin concentration and  
366 measure again.

367  
368 2.3.8.2. If there are not enough counts of single molecules measured (at least 2500-3500 for a  
369 6000-frame video with the regular field of view), increase the septin concentration and measure  
370 again.

371  
372 2.4. Direct imaging of septin complexes *via* negative stain transmission electron microscopy

373  
374 2.4.1. Dilute samples to a concentration of about 50 nM in septin buffer and prepare the staining  
375 solution (use either 2% uranyl formate or uranyl acetate in I-water).

376  
377 NOTE: Uranyl formate must be prepared fresh.

378  
379 2.4.2. Pipette 4  $\mu\text{L}$  of diluted septins onto a glow discharged electron microscopy grid and  
380 incubate for 30 s.

381  
382 2.4.3. Remove most of the protein solution using a filter paper and wash the grid twice with  
383 septin buffer and once with I-water to remove loosely adsorbed septins.

384  
385 2.4.4. Stain with 2% uranyl acetate or uranyl formate solution in I-water for 1 min, absorb the  
386 staining solution with a filter paper and air-dry the grid for a few minutes.

387  
388 2.4.5. Screen the grid using a properly aligned transmission electron microscope to search for  
389 regions of enhanced stain and collect about 100 images within these selected areas.

390  
391 2.4.6. Collect images at a magnification of at least 50,000 to obtain a pixel size of about 2  $\text{\AA}$  per  
392 pixel and with a defocus varying from  $-1$  to  $-2$   $\mu\text{m}$ . Use an acceleration voltage of 200 kV.  
393 Preferentially use an automated procedure to collect the data, which will depend on the  
394 acquisition software available.

395  
396 2.4.7. Perform 2D image processing using dedicated software  
397  
398 2.4.7.1. Box out at least 2000 particles using a dedicated software<sup>46</sup>.  
399  
400 2.4.7.2. Perform two-dimensional alignment and classification iteratively, until classes are  
401 obtained without further improvement. The first alignment and classification step should be  
402 reference-free to avoid any bias in the classification.  
403  
404 2.4.7.3. Use the averages obtained from the first reference-free classification as new references  
405 to carry out an extra round of classification. Repeat this process iteratively until no further  
406 improvement is achieved. Each class should be based on 50 to 100 picked particles and individual  
407 subunits should be clearly visible. Different software tools can be used (Spider, Eman or Relion)<sup>46-</sup>  
408 <sup>48</sup>.

### 410 **3. Septin functional quality control *via* polymerization analysis.**

411  
412 NOTE: The functionality quality control consists of a set of imaging techniques that allow for the  
413 detection of of polymerized septin complexes. Below, unlabelled septins are referred as “dark”  
414 septins and the buffer used for polymerizing unlabelled septins is referred as "dark" septin  
415 polymerization buffer (SPB).

#### 416 417 3.1. Septin bundle imaging *via* fluorescence microscopy

418  
419 3.1.1. Prepare the 5x fluoSPB (**Table 2**) and a septin mix consisting of 90% dark septin and 10%  
420 msfGFP-septin at six times higher concentration than the desired final concentration in septin  
421 buffer + 1 mM DTT. A typical concentration for this assay is 300 nM, and, therefore, the  
422 concentration is 1800 nM for this mix.

423  
424 3.1.2. Polymerize the septin by mixing, in this specific order, I-water (enough to top up to the  
425 final desired volume), 20% 5xfluoSPB (giving a final dilution of 1:5), 0.05  $\mu$ M PCD, and 16.67%  
426 septin mix (giving a final dilution of 1:6). For 10  $\mu$ L, mix 6.23  $\mu$ L of I-water, 2  $\mu$ L of 5xfluoSPB, 0.1  
427  $\mu$ L of PCD (with a stock of 5  $\mu$ M), and 1.67  $\mu$ L of septin mix. Incubate this mix for at least 30 min  
428 at room temperature.

429  
430 3.1.3. Add the samples to an imaging chamber washed with fluoSPB (**Table 2**) and image the  
431 septin bundles. PLL-PEG passivated flow channels as described in<sup>10,32</sup> work well for this  
432 experiment.

#### 433 434 3.2. Septin bundle imaging *via* negative stain transmission electron microscopy

435  
436 3.2.1. Prepare the 5x darkSPB (**Table 2**) and a septin mix consisting of 100% dark septin at six  
437 times higher concentration than the desired final concentration in septin buffer + 1 mM DTT. A

438 typical concentration for this assay is 300 nM, and, therefore, the concentration is 1800 nM for  
439 this mix.

440  
441 3.2.2. Polymerize the septin by mixing, in this specific order, I-water (enough to top up to the  
442 final desired volume), 20% 5xdarkSPB, and 16.67% septin mix. For 5  $\mu$ L, mix 3.16  $\mu$ L of I-water, 1  
443  $\mu$ L of 5xfluoSPB, and 0.83  $\mu$ L septin mix. Incubate this mix for at least 30 min at room  
444 temperature.

445  
446 3.2.3. Add 3-5  $\mu$ L of sample to a glow discharged electron microscopy grid and incubate for 1  
447 min. Then, wash the grid twice with darkSPB (**Table 2**) by absorbing the liquid with a filter paper  
448 and adding a drop of darkSPB buffer, wash once with I-water, incubate for  $\sim$ 30 s with 2% uranyl  
449 acetate, blot the stain, and air-dry the sample for a few minutes.

450  
451 **3.2.4.** Image the septin bundles at 120 kV and magnifications between 5,000x and 60,000x with  
452 a defocus of between 1 and 2  $\mu$ m.

453  
454 **REPRESENTATIVE RESULTS:**  
455 As mentioned in the protocol, 5 L of *E. coli* cells co-transformed with the two septin expressing  
456 plasmids were grown and the expression of septins was induced by adding IPTG. After 3 h, the  
457 cells were collected by centrifugation, resuspended in lysis buffer, and lysed by sonication. The  
458 lysate was then clarified by centrifugation and the clarified solution was applied to a HisTrap  
459 column (**Figure 2A**). After the first purification, the septin-containing fractions were pooled and  
460 applied onto a StrepTrap column (**Figure 2B**). This typically yields around 3-5 mL of  $\sim$ 1  $\mu$ M of  
461 septin complex. Before pooling the septin-containing fractions, a denaturing gel can be used to  
462 check for the integrity of the septin subunits and an equimolar stoichiometric ratio between the  
463 different septin subunits forming the complex. (**Figure 3A**). If the gel shows similarly intense  
464 bands corresponding to the molecular weights (**Table 3**) of the septin subunits, the protocol can  
465 be continued. If not, it is recommended to start the protocol again. In the example shown for  
466 human septin octamer with SEPT9\_i1, **Figure 3A** clearly shows bands corresponding to SEPT9\_i1,  
467 SEPT6, SEPT7, and SEPT2 (in the order from top to bottom) with similar intensity; the 99%  
468 confidence interval of the normalized intensity was  $1.128 \pm 0.048$  for SEPT2,  $1.092 \pm 0.034$  for  
469 SEPT6,  $1.108 \pm 0.040$  for SEPT7, and  $1.067 \pm 0.029$  for SEPT9. If SEPT2 is tagged with msfGFP, it will  
470 shift up, very close below SEPT9\_i1. Depending on the electrophoresis system used and the  
471 presence of the C-terminal TEV-Strep tag for SEPT7 (which makes it migrate more slowly than  
472 untagged SEPT7), the SEPT7 and SEPT6 bands sometimes merge due to their comparable  
473 molecular weights. The next step is to pool the fractions and dialyze them against septin buffer  
474 with DTT. After the dialysis, if the concentration is too low ( $<2 \mu$ M) or a higher concentration is  
475 needed for the experiments, a concentration step can be included as described in the protocol.  
476 Concentrations below 1  $\mu$ M usually indicate the bad functional quality of the septins. A final  
477 septin complex concentration between 3.5  $\mu$ M and 7  $\mu$ M works well for most *in vitro* assays.  
478 These concentrations are usually obtained when the volume after concentration reaches 0.5-1  
479 mL.

480  
481 [Place **Figure 2** here]

482  
483 To continue with the quality control, a native electrophoresis, as described in the protocol, was  
484 performed (**Figure 3B**). In the gels, a major band corresponding to the intact hetero-oligomers  
485 and usually a minor band corresponding to trimers or tetramers can be observed. Human  
486 hexamers are found a little bit above the 242 kDa marker band while octamers are found above  
487 the 480 kDa band, above their calculated molecular mass. The location of these bands was  
488 checked by western blot analysis of eukaryotic cell extracts<sup>32</sup>. Tagging with msfGFP couples each  
489 SEPT2 with a msfGFP protein. This causes an increase in the molecular weight of septin complexes  
490 of 53.4 kDa (26.7kDa per msGFP molecule). Nevertheless, on the native electrophoresis gel, the  
491 apparent molecular weight of the msfGFP-tagged complexes is indistinguishable from that of the  
492 untagged complexes.

493  
494 A complementary technique to test whether the septin complexes are intact is mass photometry  
495 by iSCAT microscopy. iSCAT monitors the light scattering of molecules landing on a glass slide  
496 amplified by interference with reference light, typically the reflection of the laser on the bottom  
497 of the glass slide. Then, a background subtraction approach is used to give contrast to the  
498 particles. Due to this correction, the signal shows positive and negative values depending on  
499 whether the particles land on the glass or move away from it<sup>49</sup>. The detected signal is directly  
500 proportional to the molecular weight of proteins<sup>50</sup>. Therefore, a signal-to-mass calibration with  
501 a mass standard can determine the mass of sample proteins. **Figure 3C** shows an example of  
502 human septin octamers containing SEPT9\_i1. Most of the detected single particles (~50%) are of  
503 a molecular weight expected for complete octamers containing SEPT9\_i1 (423 kDa) (**Figure 3C**).  
504 There are also particles with masses between 150 and 300 kDa, but no clear peak is observed,  
505 indicating the possible presence of other septin species in low abundance. Similarly, most of the  
506 detected single particles for mEGFP-tagged *Drosophila* hexamers are of a molecular weight  
507 expected for intact hexamers (361 kDa) (**Figure 3D**). An additional clear peak at 241 kDa indicates  
508 the presence of stable tetramers containing two Peanut proteins, one DSep1, and one mEGFP-  
509 DSep2. Finally, both the human and the fly septin complexes show a peak around 80 kDa, that  
510 could be a mix of monomers and dimers, possibly amplified by a trace of DTT or any other small  
511 molecule that aggregates showing a peak in the positive side of the plot<sup>45</sup>.

512  
513 [Place **Figure 3** here]

514  
515 Given that both native gels and iSCAT provide ensemble-averaged information only, class  
516 averaging of transmission electron microscopy images of single septin oligomers was used to  
517 check the integrity and purity of the complexes by direct visualization. In TEM images of septin  
518 complexes in septin buffer, rods of 24 nm (hexamers) or 32 nm (octamers) in length can be  
519 observed. An example of a human septin octamer containing SEPT9\_i1 can be seen in **Figure 3E**.  
520 When class averaging them, each of the subunits can be observed and counted, as seen for the  
521 msfGFP-tagged human octamer with SEPT9\_i1 in **Figure 3F**. In case the oligomer is fluorescently  
522 labeled, extra densities that correspond to the SEPT2-msfGFP can be observed at the end of the  
523 rods (**Figure 3F**).

524

525 The combination of the above techniques proves that octamers (or hexamers) with the correct  
526 stoichiometric ratio and high purity can be purified using the described protocol. Finally, the last  
527 quality control check is for the functionality of the septin complexes in terms of their  
528 polymerization ability. In the presence of low salt concentration (<150 mM KCl with the described  
529 buffer<sup>9</sup>), if septins are not in the presence of other proteins or negatively charged lipid  
530 membranes, they self-assemble into bundles<sup>9</sup>. Septins are prevented from polymerization by  
531 keeping them in the storage buffer which has a high (300 mM) KCl concentration. The septin  
532 hetero-oligomers are then diluted 1:6 volume ratio in a buffer of the same composition but  
533 without KCl, to achieve a final KCl concentration of 50 mM. To do fluorescence imaging, this  
534 buffer is complemented with an oxygen scavenging system, to protect from photobleaching, and  
535 with a blinking suppressor. In TIRF microscopy, small clusters of proteins can be observed within  
536 the shallow TIRF field (~100 nm; **Figure 4A,B**). On a confocal microscope, large clusters of  
537 filamentous structures can be seen floating higher up in solution (**Figure 4C**). Finally, with TEM,  
538 small bundles of septin (**Figure 4D**) corresponding to the clusters observed by TIRF and large  
539 bundles (**Figure 4E**) corresponding to the structures observed by confocal microscopy can be  
540 observed. The insets of **Figure 4D,E** reveal that both types of structures consist of long and thin  
541 filaments that run in parallel, forming bundles with tapered ends. Together, the fluorescence and  
542 TEM images prove that the purified septin complexes can polymerize into filaments, which in  
543 turn self-assemble into bundles.

544

545 [Place **Figure 4** here]

546

#### 547 **FIGURE AND TABLE LEGENDS:**

548 **Figure 1: Purification strategy.** (A) Schematics of the septin hetero-oligomers that exist in human  
549 (left) and *Drosophila* (right) cells. Numbers denote septin subunits from the indicated groups,  
550 and P denotes Peanut. Note that human SEPT9 can be any of its isoforms. The septin subunits  
551 have an asymmetric shape and are longitudinally associated with two distinct interfaces, the  
552 NC:NC and the G:G interface, as denoted by NC and G, respectively, on top of the human  
553 hexamer. (B and C) Schematic illustration of the two-step chromatography strategy, shown for  
554 human septin hexamers (B) and octamers (C). H indicates the his-tags while S indicates the Strep-  
555 II-tags.

556

557 **Figure 2: Example chromatograms corresponding to the purification of dark human septin**  
558 **octamers\_9i1.** (A) HisTrap column chromatogram. After the septin elution peak, the absorbance  
559 does not go back to zero, likely due to the presence of imidazole in the buffer. Pooled fraction  
560 went from the start of the elution peak until the absorbance stabilized at around 250 mL. (B)  
561 StrepTrap column chromatogram. Pooled fraction went from the start of the elution peak until  
562 the absorbance went back to around 0 at 50 mL.

563

564 **Figure 3: Examples of results of the oligomer quality control.** (A) Example of denaturing gel  
565 showing different fractions of the elution peak from the purification of dark human septin  
566 octamers\_9i1. (B) Example of native electrophoresis of different septin complexes. (C,D)  
567 Different examples of histogram results of mass photometry at 12.5 nM of septin complexes: (C)  
568 dark human septin octamers\_9i1 and (D) DSep1-msfGFP *Drosophila* septin hexamers. Lines are

569 Gaussian fits. (E) TEM image of 25 nM dark human septin octamers\_9i1 in septin buffer. Scale  
570 bar = 200 nm. (F) Class average image of SEPT2-msfGFP human septin octamers\_9i1. The msfGFP  
571 tags are visible as fuzzy densities on the two ends. Scale bar = 10 nm. Panels E and F are adapted  
572 from Iv et al.<sup>10</sup> with permission.

573  
574 **Figure 4: Examples of results of the polymerization ability quality control.** (A) TIRF image of 300  
575 nM human septin hexamers (10% msfGFP-labelled hexamers) in fluoSPB. (B) TIRF image of 300  
576 nM human septin octamers containing SEPT9\_i1 (10% msfGFP-labelled octamers9\_i1) in fluoSPB.  
577 (C) Confocal maximum-intensity projections of Z-stacks across ~30  $\mu\text{m}$  with 0.5  $\mu\text{m}$  of spacing of  
578 300 nM human septin octamers\_9i3 in fluoSPB. (A-C) Scale bar = 10  $\mu\text{m}$  and inverted grayscale.  
579 (D,E) Example TEM images of small (D) and large (E) bundles of human septin octamers\_9i1 in  
580 darkSPB. Insets show regions where clear filaments running parallel within the bundle can be  
581 observed. Scale bars = 500 nm. Panels C-E are adapted from Iv et al.<sup>10</sup> with permission.

582  
583 **Table 1: List of plasmids.** Plasmids to purify septin oligomers following this protocol. All plasmids  
584 have been deposited in Addgene (first column).

585  
586 **Table 2: List of buffers.** Buffer compositions used for the purification and quality control of septin  
587 oligomers.

588  
589 **Table 3: Molecular weights and extinction coefficients.** List of molecular weights (MW) and  
590 optical extinction coefficients ( $\epsilon$ ) at a wavelength of 280 nm calculated with ProtParam based on  
591 the sequences of the complex assuming a linear fusion of the septin subunits, the different septin  
592 complexes, and unique septin subunits (only MW) that can be purified with the plasmids listed  
593 in **Table 1**.

594  
595 **DISCUSSION:**  
596 The method described here allows for the robust purification and quality control of pre-formed  
597 septin hetero-oligomers. Some issues of vital importance must be conducted for the correct  
598 application of the method. First, during the elution steps in the chromatographic separations, it  
599 is important to use the recommended (or lower) flow rate to minimize the dilution of the septin  
600 complexes. Additionally, to maximize the recovery of protein during the final concentration step,  
601 the concentrator column is oriented in such a way that the solution is not pushed against the  
602 filter (when there is only a filter on one side). If the solution goes directly to the filter, the protein  
603 sticks much more to it, substantially decreasing the final yield. It is also important to consider  
604 that the concentration step is not always necessary. Picking fractions only from a narrow range  
605 around the peak in the chromatogram usually gives a high enough stock concentration (>3000  
606 nM) for many reconstitution applications (which usually operate between 10 and 300 nM).  
607 Finally, for the quality control of the functionality of the septin complexes by fluorescence  
608 microscopy, it is important to correctly passivate the surface of the microscopy slides, since  
609 septin complexes avidly stick to glass. Passivation of the glass slides can be done either *via* PLL-  
610 PEG functionalization or by the formation of neutral (100% DOPC) supported lipid bilayers<sup>11,32</sup>.

611

612 Compared to the original purification protocol first described in Iv et al.<sup>10</sup>, there is a change in  
613 the buffer compositions (**Table 2**): the concentration of MgCl<sub>2</sub> has been reduced from 5 to 2 mM  
614 and the concentration and pH of Tris-HCl have been reduced from 50 to 20 mM and from 8 to  
615 7.4, respectively. These changes were made to make the buffer conditions compatible with  
616 studies of the interactions of human septins with lipid bilayers, actin filaments, and  
617 microtubules<sup>10,11,32</sup>. This is because the authors form supported lipid bilayers and polymerize  
618 actin in the F-buffer, whose composition is identical to that of darkSPB, apart from the presence  
619 of ATP in the F-buffer. The buffer change has not produced any changes in the quality or lifetime  
620 of the purified septins compared to the original buffers.

621  
622 This method of purification still has several limitations. First, different purification attempts can  
623 vary in yield (0.5-1 mL of 2-5 μM of septin complexes) and functional quality, as checked by the  
624 bundle formation ability of the purified septin complexes. That is why it is very important to  
625 consistently perform the quality checks described in this paper. Controlling very well the times  
626 of expression and the optical density of the bacterial culture can help mitigate the difference in  
627 yield. Second, this purification pipeline cannot distinguish between trimers and hexamers, or  
628 between tetramers and octamers (**Figure 1B**). However, the quality control experiments can be  
629 used to prove that the majority of septin complexes are in their long oligomer form. In case an  
630 even narrow oligomer size distribution is required, size exclusion chromatography can be  
631 inserted in between steps 1.6 and 1.7 of the purification protocol. This optional step, however,  
632 dramatically decreases the yield and it is not recommended unless it is strictly needed. A last,  
633 more fundamental, limitation comes from the use of *E. coli* as an expression system for  
634 recombinant septin complexes. Naturally, this system does not allow for post-translational  
635 modifications (PTMs) which have been reported in animal cells, such as phosphorylation,  
636 acetylation, and sumoylation<sup>6,51-53</sup>. These posttranslational modifications could be added by  
637 implementing a similar purification strategy in insect or human cells. Furthermore, this paper  
638 only discussed the reconstitution of septins by themselves, but studies in cells indicate that  
639 regulatory proteins such as proteins from the Borg family<sup>54,55</sup> and anillin<sup>24,25,56</sup> can have  
640 substantial yet poorly understood effects on the assembly and functions of septins and are,  
641 therefore, important to eventually incorporate in *in vitro* studies. Protocols for the purification  
642 of Borg proteins and anillin have been reported<sup>54,57</sup>.

643  
644 The septin purification protocol reported here offers a standardized way to purify septins in their  
645 oligomer form with the correct subunit stoichiometry, offering an important advance over many  
646 earlier *in vitro* studies relying on single septin subunits. Even though some septins in specific  
647 contexts can act as a single subunit<sup>2</sup>, the current body of literature strongly suggests that, in  
648 animal cells, septins mostly function in complexes<sup>9,58</sup>. Therefore, the use of pre-formed hetero-  
649 oligomers, such as the ones described in this paper and others<sup>10,11,18,32,35-37</sup>, is of great importance  
650 to study the structural and biophysical properties of septins *via in vitro* reconstitution to dissect  
651 their functions in the cell. Furthermore, septins are self-assembling proteins with many  
652 interaction partners, including the membrane and the cytoskeleton, which makes them of great  
653 interest for bottom-up synthetic biology<sup>59-61</sup> and studies of protein-induced changes in  
654 membrane biophysical properties such as curvature<sup>42,62,63</sup>.

655



656 **ACKNOWLEDGEMENTS:**

657 We thank Cecilia de Agrela Pinto, Tomás de Garay, and Katharina Häußermann for their  
658 assistance with mass photometry (iSCAT) experiments; Arjen Jakobi and Wiel Evers for their help  
659 with TEM; Lucia Baldauf for her assistance with TIRF; Pascal Verdier-Pinard for his advice  
660 concerning native electrophoresis; and Agata Szuba and Marjolein Vinkenoog for their help in  
661 setting up the *Drosophila* septin purification efforts. This research received funding from the  
662 Netherlands Organization for Scientific Research (NWO/OCW) through the ‘BaSyC—Building a  
663 Synthetic Cell’ Gravitation grant (024.003.019) and from the Agence Nationale pour la Recherche  
664 (ANR grant ANR-17-CE13-0014; SEPTIMORF).

665  
666 **DISCLOSURES:**

667 The authors declare no competing or financial interests.

668  
669 **REFERENCES:**

- 670 1. Mostowy, S. & Cossart, P. Septins: The fourth component of the cytoskeleton. *Nature*  
671 *Reviews Molecular Cell Biology* **13**, 183–194 (2012).
- 672 2. Shuman, B. & Momany, M. Septins From Protists to People. *Frontiers in Cell and*  
673 *Developmental Biology* **9**, 3802 (2022).
- 674 3. Bridges, A. A. & Gladfelter, A. S. Septin form and function at the cell cortex. *Journal of*  
675 *Biological Chemistry* **290**, 17173–17180 (2015).
- 676 4. Smith, C. *et al.* Septin 9 Exhibits Polymorphic Binding to F-Actin and Inhibits Myosin and  
677 Cofilin Activity. *Journal of Molecular Biology* **427**, 3273–3284 (2015).
- 678 5. Gilden, J. K., Peck, S., Chen, Y. C. M. & Krummel, M. F. The septin cytoskeleton facilitates  
679 membrane retraction during motility and blebbing. *Journal of Cell Biology* **196**, 103–114 (2012).
- 680 6. Marquardt, J., Chen, X. & Bi, E. Architecture, remodeling, and functions of the septin  
681 cytoskeleton. *Cytoskeleton* (2018). doi:10.1002/cm.21475
- 682 7. Van Ngo, H. & Mostowy, S. Role of septins in microbial infection. *Journal of Cell Science*  
683 **132**, (2019).
- 684 8. Fung, K. Y. Y., Dai, L. & Trimble, W. S. Cell and molecular biology of septins. in *International*  
685 *Review of Cell and Molecular Biology* **310**, 289–339 (Academic Press, 2014).
- 686 9. Kinoshita, M., Field, C. M., Coughlin, M. L., Straight, A. F. & Mitchison, T. J. Self- and actin-  
687 templated assembly of mammalian septins. *Developmental Cell* **3**, 791–802 (2002).
- 688 10. Iv, F. *et al.* Insights into animal septins using recombinant human septin octamers 2 with  
689 distinct SEPT9 isoforms. *Journal of Cell Science* 2021.01.21.427698 (2021).  
690 doi:10.1242/JCS.258484
- 691 11. Szuba, A. *et al.* Membrane binding controls ordered self-assembly of animal septins. *eLife*  
692 **10**, (2021).
- 693 12. Kinoshita, M. Assembly of Mammalian Septins. *Journal of Biochemistry* **134**, 491–496  
694 (2003).
- 695 13. Connolly, D. *et al.* Septin 9 isoform expression, localization and epigenetic changes during  
696 human and mouse breast cancer progression. *Breast Cancer Research* **13**, R76 (2011).
- 697 14. Connolly, D. *et al.* Septin 9 amplification and isoform-specific expression in peritumoral  
698 and tumor breast tissue. *Biological Chemistry* **395**, 157–167 (2014).
- 699 15. Estey, M. P., Di Ciano-Oliveira, C., Froese, C. D., Bejide, M. T. & Trimble, W. S. Distinct roles

700 of septins in cytokinesis: SEPT9 mediates midbody abscission. *Journal of Cell Biology* **191**, 741–  
701 749 (2010).

702 16. John, C. M. *et al.* The *Caenorhabditis elegans* septin complex is nonpolar. *EMBO Journal*  
703 **26**, 3296–3307 (2007).

704 17. Field, C. M. *et al.* A purified *Drosophila* septin complex forms filaments and exhibits  
705 GTPase activity. *Journal of Cell Biology* **133**, 605–616 (1996).

706 18. Bertin, A. *et al.* *Saccharomyces cerevisiae* septins: Supramolecular organization of  
707 heterooligomers and the mechanism of filament assembly. *Proceedings of the National Academy*  
708 *of Sciences of the United States of America* **105**, 8274–8279 (2008).

709 19. Sellin, M. E., Sandblad, L., Stenmark, S. & Gullberg, M. Deciphering the rules governing  
710 assembly order of mammalian septin complexes. *Molecular Biology of the Cell* **22**, 3152–3164  
711 (2011).

712 20. Akil, A. *et al.* Septin 9 induces lipid droplets growth by a phosphatidylinositol-5-phosphate  
713 and microtubule-dependent mechanism hijacked by HCV. *Nature Communications* **7**, 12203  
714 (2016).

715 21. Tanaka-Takiguchi, Y., Kinoshita, M. & Takiguchi, K. Septin-Mediated Uniform Bracing of  
716 Phospholipid Membranes. *Current Biology* **19**, 140–145 (2009).

717 22. Omrane, M. *et al.* Septin 9 has two polybasic domains critical to septin filament assembly  
718 and Golgi integrity. *iScience* 138–153 (2019). doi:10.1016/j.isci.2019.02.015

719 23. Carim, S. C., Kechad, A. & Hickson, G. R. X. Animal Cell Cytokinesis: The Rho-Dependent  
720 Actomyosin-Anilloseptin Contractile Ring as a Membrane Microdomain Gathering, Compressing,  
721 and Sorting Machine. *Frontiers in Cell and Developmental Biology* **8**, (2020).

722 24. Amine, N. El, Kechad, A., Jananji, S. & Hickson, G. R. X. Opposing actions of septins and  
723 Sticky on Anillin promote the transition from contractile to midbody ring. *Journal of Cell Biology*  
724 **203**, 487–504 (2013).

725 25. Renshaw, M. J., Liu, J., Lavoie, B. D. & Wilde, A. Anillin-dependent organization of septin  
726 filaments promotes intercellular bridge elongation and Chmp4B targeting to the abscission site.  
727 *Open Biology* **4**, 130190 (2014).

728 26. Vogt, E. T. *et al.* The ultrastructural organization of actin and myosin II filaments in the  
729 contractile ring: new support for an old model of cytokinesis. *Molecular Biology of the Cell* **28**,  
730 613–623 (2017).

731 27. Mavrakis, M. *et al.* Septins promote F-actin ring formation by crosslinking actin filaments  
732 into curved bundles. *Nature Cell Biology* **16**, 322–334 (2014).

733 28. Karasmanis, E. P. *et al.* A Septin Double Ring Controls the Spatiotemporal Organization of  
734 the ESCRT Machinery in Cytokinetic Abscission. *Current Biology* **29**, 2174–2182.e7 (2019).

735 29. Hagiwara, A. *et al.* Submembranous septins as relatively stable components of actin-  
736 based membrane skeleton. *Cytoskeleton* **68**, 512–525 (2011).

737 30. Calvo, F. *et al.* Cdc42EP3/BORG2 and Septin Network Enables Mechano-transduction and  
738 the Emergence of Cancer-Associated Fibroblasts. *Cell Reports* **13**, 2699–2714 (2015).

739 31. Salameh, J., Cantaloube, I., Benoit, B., Poüs, C. & Baillet, A. Cdc42 and its BORG2 and  
740 BORG3 effectors control the subcellular localization of septins between actin stress fibers and  
741 microtubules. *Current Biology* (2021). doi:10.1016/J.CUB.2021.07.004

742 32. Kuzmić, M. *et al.* Septin-microtubule association via a motif unique to isoform 1 of septin  
743 9 tunes stress fibers. *Journal of Cell Science* **135**, (2022).

744 33. Shindo, A. *et al.* Septin-dependent remodeling of cortical microtubule drives cell  
745 reshaping during epithelial wound healing. *Journal of Cell Science* **131**, jcs212647 (2018).

746 34. Hu, Q., Nelson, W. J. & Spiliotis, E. T. Forchlorfenuron alters mammalian septin assembly,  
747 organization, and dynamics. *Journal of Biological Chemistry* **283**, 29563–29571 (2008).

748 35. Mavrakis, M., Tsai, F. C. & Koenderink, G. H. Purification of recombinant human and  
749 *Drosophila* septin hexamers for TIRF assays of actin–septin filament assembly. *Methods in Cell*  
750 *Biology* **136**, 199–220 (2016).

751 36. Nakos, K., Radler, M. R. & Spiliotis, E. T. Septin 2/6/7 complexes tune microtubule plus-  
752 end growth and EB1 binding in a concentration- and filament-dependent manner. *Molecular*  
753 *Biology of the Cell* **30**, 2913–2928 (2019).

754 37. Kaplan, C. *et al.* Absolute Arrangement of Subunits in Cytoskeletal Septin Filaments in  
755 Cells Measured by Fluorescence Microscopy. *Nano Letters* **15**, 3859–3864 (2015).

756 38. Castro, D. K. S. V. *et al.* A complete compendium of crystal structures for the human SEPT3  
757 subgroup reveals functional plasticity at a specific septin interface. *IUCr* **7**, 462–479 (2020).

758 39. Jiao, F., Cannon, K. S., Lin, Y.-C., Gladfelter, A. S. & Scheuring, S. The hierarchical assembly  
759 of septins revealed by high-speed AFM. *Nature Communications* **2020** **11**, 1–13 (2020).

760 40. Bertin, A. *et al.* Phosphatidylinositol-4,5-bisphosphate Promotes Budding Yeast Septin  
761 Filament Assembly and Organization. *Journal of Molecular Biology* **404**, 711–731 (2010).

762 41. Bridges, A. A., Jentsch, M. S., Oakes, P. W., Occhipinti, P. & Gladfelter, A. S. Micron-scale  
763 plasma membrane curvature is recognized by the septin cytoskeleton. *Journal of Cell Biology* **213**,  
764 23–32 (2016).

765 42. Beber, A. *et al.* Membrane reshaping by micrometric curvature sensitive septin filaments.  
766 *Nature Communications* **10**, 420 (2019).

767 43. Zhou, R., Shi, Y. & Yang, G. Expression, Purification, and Enzymatic Characterization of  
768 Intramembrane Proteases. in *Methods in Enzymology* **584**, 127–155 (Academic Press, 2017).

769 44. Diebold, M. L., Fribourg, S., Koch, M., Metzger, T. & Romier, C. Deciphering correct  
770 strategies for multiprotein complex assembly by co-expression: Application to complexes as large  
771 as the histone octamer. *Journal of Structural Biology* **175**, 178–188 (2011).

772 45. Lebedeva, M. A., Palmieri, E., Kukura, P. & Fletcher, S. P. Emergence and Rearrangement  
773 of Dynamic Supramolecular Aggregates Visualized by Interferometric Scattering Microscopy. *ACS*  
774 *Nano* **14**, 11160–11168 (2020).

775 46. Ludtke, S. J., Baldwin, P. R. & Chiu, W. EMAN: Semiautomated Software for High-  
776 Resolution Single-Particle Reconstructions. *Journal of Structural Biology* **128**, 82–97 (1999).

777 47. Zivanov, J. *et al.* New tools for automated high-resolution cryo-EM structure  
778 determination in RELION-3. *eLife* **7**, (2018).

779 48. Frank, J. *et al.* SPIDER and WEB: Processing and visualization of images in 3D electron  
780 microscopy and related fields. *Journal of Structural Biology* **116**, 190–199 (1996).

781 49. Young, G. & Kukura, P. Interferometric Scattering Microscopy. *Annual Review of Physical*  
782 *Chemistry* **70**, 301–322 (2019).

783 50. Young, G. *et al.* Quantitative mass imaging of single biological macromolecules. *Science*  
784 **360**, 423–427 (2018).

785 51. Hernández-Rodríguez, Y. & Momany, M. Posttranslational modifications and assembly of  
786 septin heteropolymers and higher-order structures. *Current Opinion in Microbiology* **15**, 660–668  
787 (2012).

788 52. Ribet, D. *et al.* SUMOylation of human septins is critical for septin filament bundling and  
789 cytokinesis. *Journal of Cell Biology* **216**, 4041–4052 (2017).

790 53. Sinha, I. *et al.* Cyclin-Dependent Kinases Control Septin Phosphorylation in *Candida*  
791 *albicans* Hyphal Development. *Developmental Cell* **13**, 421–432 (2007).

792 54. Sheffield, P. J. *et al.* Borg/Septin interactions and the assembly of mammalian septin  
793 heterodimers, trimers, and filaments. *Journal of Biological Chemistry* **278**, 3483–3488 (2003).

794 55. Joberty, G. *et al.* Borg proteins control septin organization and are negatively regulated  
795 by Cdc42. *Nature Cell Biology* **3**, 861–866 (2001).

796 56. Chen, X., Wang, K., Svitkina, T. & Bi, E. Critical Roles of a RhoGEF-Anillin Module in Septin  
797 Architectural Remodeling during Cytokinesis. *Current Biology* **30**, 1477–1490.e3 (2020).

798 57. Kučera, O. *et al.* Anillin propels myosin-independent constriction of actin rings. *Nature*  
799 *Communications* **2021 12:1** **12**, 1–12 (2021).

800 58. Hsu, S. C. *et al.* Subunit composition, protein interactions, and structures of the  
801 mammalian brain sec6/8 complex and septin filaments. *Neuron* **20**, 1111–1122 (1998).

802 59. Olivi, L. *et al.* Towards a synthetic cell cycle. *Nature Communications* **12**, 1–11 (2021).

803 60. Hürtgen, D., Härtel, T., Murray, S. M., Sourjik, V. & Schwille, P. Functional Modules of  
804 Minimal Cell Division for Synthetic Biology. *Advanced Biosystems* **1800315**, 1–9 (2019).

805 61. Jia, H. & Schwille, P. Bottom-up synthetic biology: reconstitution in space and time.  
806 *Current Opinion in Biotechnology* **60**, 179–187 (2019).

807 62. Cannon, K. S., Woods, B. L., Crutchley, J. M. & Gladfelter, A. S. An amphipathic helix  
808 enables septins to sense micrometer-scale membrane curvature. *The Journal of Cell Biology* **218**,  
809 1128–1137 (2019).

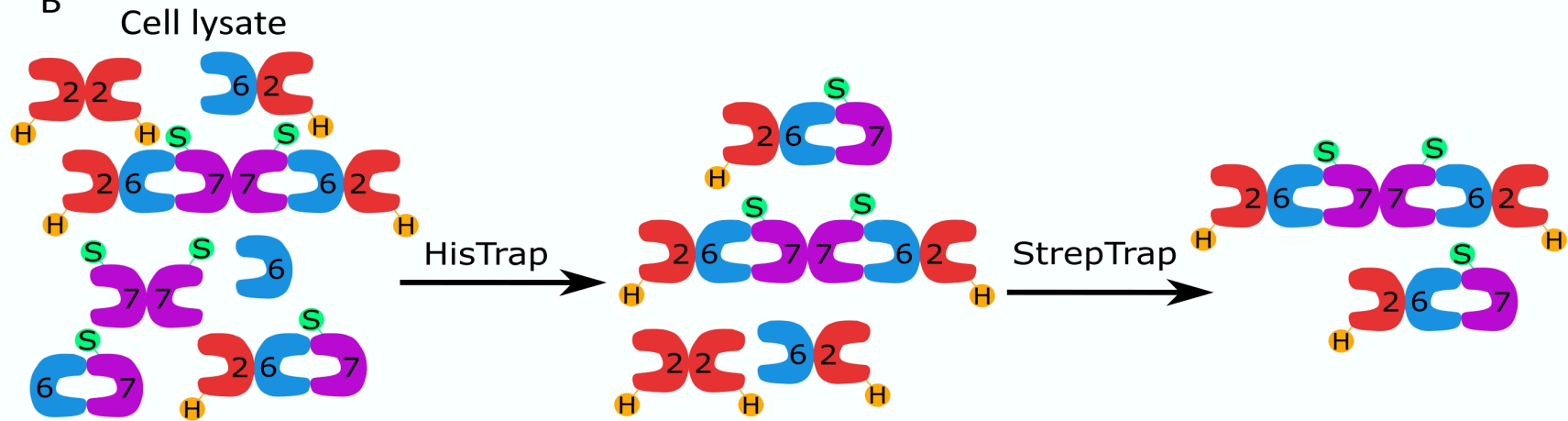
810 63. Lobato-Márquez, D. & Mostowy, S. Septins recognize micron-scale membrane curvature.  
811 *Journal of Cell Biology* **213**, 5–6 (2016).

812

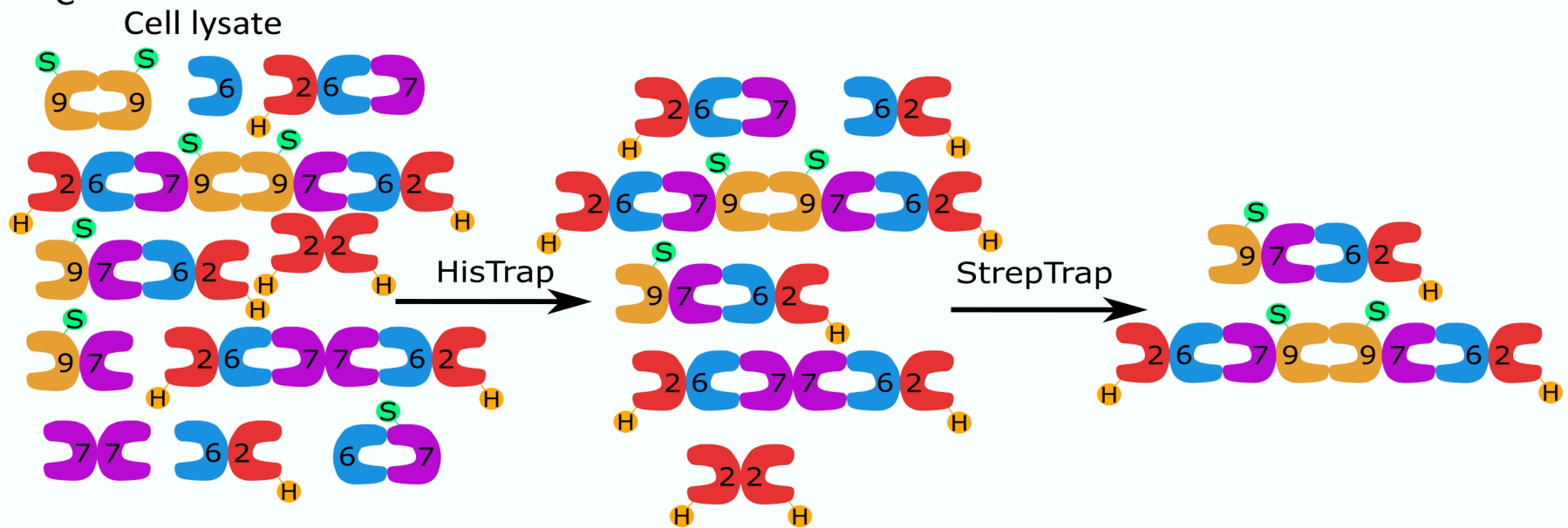
A

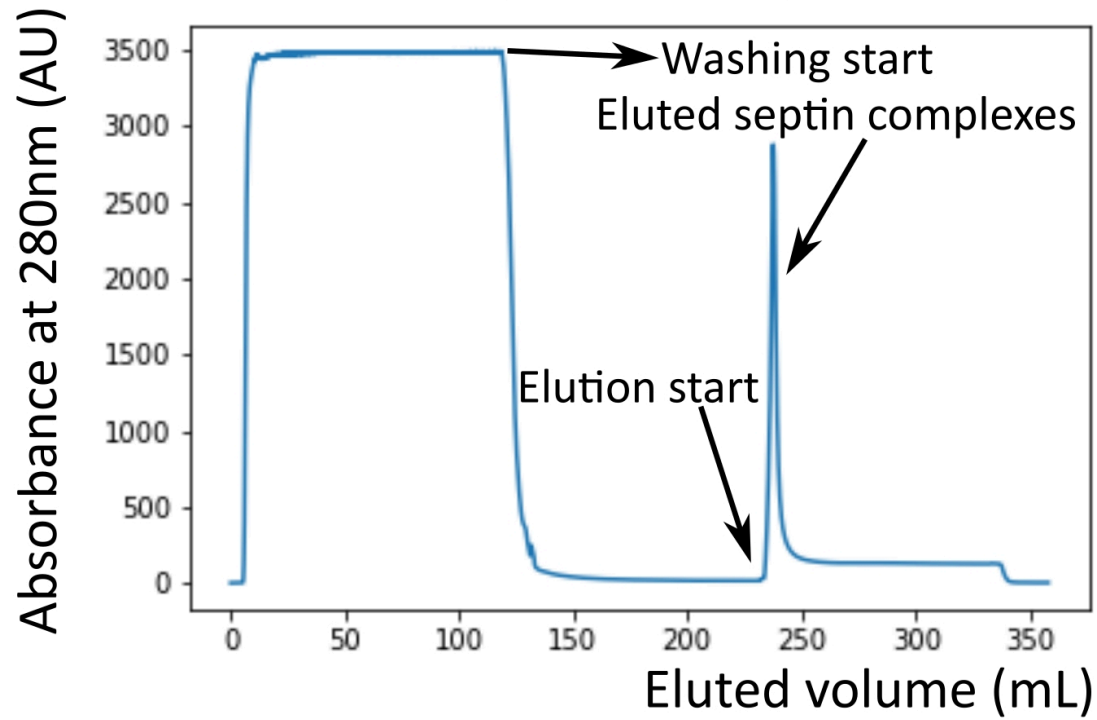


B



C



**A****HisTrap Chromatogram****B****StrepTrap Chromatogram**